Research Square

Preprints are preliminary reports that have not undergone peer review.
They should not be considered conclusive, used to inform clinical practice,
or referenced by the media as validated information.

Integrated transcriptomic and proteomic profiling reveals dynamic liver injury and molecular responses during Echinococcus granulosus infection in rats

Laizhen Liu
Xinjiang Agricultural University
Xiaoyan Ma
Xinjiang Uygur Autonomous Region Animal Disease Prevention and Control Center
Weilu Li
Xinjiang Agricultural University
Jiuge Zhang
Xinjiang Agricultural University
Eli Zulhuma
Xinjiang Agricultural University
Shaohua Zhai
183099169370163.com

Xinjiang Agricultural University

Research Article

Keywords: Echinococcus granulosus, cystic echinococcosis, transcriptomics, proteomics, liver injury, metabolic reprogramming

Posted Date: November 17th, 2026

DOI: https://doi.org/10.21203/rs.3.rs-11551848/v1

License: This work is licensed under a Creative Commons Attribution 4.0 International License.
Read Full License

Additional Declarations: No competing interests reported.

Integrated transcriptomic and proteomic profiling reveals dynamic liver injury and molecular responses during *Echinococcus granulosus* infection in rats

Laizhen Liu[1,2†], Xiaoyan Ma[3], Weilu Li[1,2], Jiuge Zhang[1,2], Zulhuma·Eli[1,2],Shaohua Zhai[1,2*,†]

1 College of Veterinary Medicine, Xinjiang Agricultural University, Urumqi 830052, China;

2 Xinjiang·Key Laboratory of New Drug Research and Development for Herbivorous (XJ-LNDRDH), Urumqi 830052, China;

3 Xinjiang Uygur Autonomous Region Animal Disease Prevention and Control Center, Urumqi, 830011, China.

*Corresponding author(s). E-mail(s): 18309916937@163.com;

Contributing authors: liu859lsqc@163.com; mxy0313@163.com; 493875203@qq.com; 1516504638@qq.com; 2530650395@qq.com; 18309916937@163.com.

†These authors contributed equally to this work.

Abstract: Cystic echinococcosis (CE) is a severe zoonotic parasitic disease in which the liver is the major target organ. Progressive growth of parasitic cysts can cause chronic liver injury and fibrosis, yet the molecular events underlying long-term parasitism and hepatic damage remain incompletely understood. In this study, we established a rat model of *Echinococcus granulosus* (*E. granulosus*) infection and integrated transcriptomic and proteomic profiling with quantitative real-time PCR (qRT-PCR), Western blotting, and immunohistochemistry (IHC) to characterize host liver responses at 1, 3, and 6 months after infection. Across the course of infection, the liver exhibited marked changes in metabolic and immune-related pathways, with prominent enrichment of pathways associated with the cell cycle, interferon signaling, and carbohydrate metabolism. Validation of selected targets revealed a time- and location-dependent pattern of Stat1 expression: strong staining was observed in inflammatory infiltrates during the early and intermediate stages, whereas expression became restricted predominantly to the fibrous cyst wall at the chronic stage. Ccnd1 also showed distinct spatiotemporal changes, shifting from hepatocyte-associated expression at earlier stages toward enrichment in the fibrous cyst wall and fibroblast-like cells at 6 months. Integrated pathway analysis identified six pathways shared across all three time points, including B-cell receptor signaling, phagosome, cytosolic DNA-sensing, cell adhesion molecules, galactose metabolism, and fructose and mannose metabolism. Collectively, these findings delineate a dynamic molecular landscape in the liver during *E. granulosus* infection and suggest coordinated remodeling of immune responses, tissue architecture, and host metabolism during the establishment of chronic infection.

Keywords: *Echinococcus granulosus*; cystic echinococcosis; transcriptomics; proteomics; liver injury; metabolic reprogramming

1 Introduction

Cystic echinococcosis (CE) is an important zoonotic parasitic disease caused by *Echinococcus granulosus* (*E. granulosus*) at the larval stage. One million people are estimated to be affected worldwide in pastoral regions[1-4]. CE is characterized by a long latent period until cyst-induced liver damages are detected in sheep with symptoms such as hepatic region pain, ascites, cough, dyspnea, emaciation, and weakness. The larval stage of *E. granulosus* can infect various organs and tissues, including the liver, lungs, spleen, kidneys, brain, and bones; however, the liver is the primary target for *E. granulosus,* accounting for ~70% of cases[5,6]. Infection with *E. granulosus* not only reduces livestock productivity and leads to the condemnation of organs at slaughter, causing severe economic losses to the livestock industry, but also threatens human health and can cause severe complications and even death[7]. Therefore, CE is both a livestock disease and an important public health problem.

Treatment of cystic echinococcosis (CE) requires individualized decision-making, and current management accordingly combines surgical removal, percutaneous aspiration-injection-reaspiration (PAIR), and benzimidazole therapy such as albendazole[8,9]. Albendazole is the cornerstone of pharmacological therapy but is often combined with surgical or interventional approaches to achieve optimal outcomes. However, recurrence, treatment-related adverse effects, and limited efficacy in advanced disease remain important challenges. A better understanding of the molecular mechanisms that permit long-term parasite survival and progressive hepatic injury is therefore needed to identify new intervention strategies.

The liver represents a major site at which *E. granulosus* larvae are retained during migration through the host circulation[9]. Parasite-derived antigens and excretory/secretory products (ESPs) can modify local immune responses and may contribute to sustained tissue injury[10]. As infection progresses, expanding cysts can exert mechanical pressure on adjacent parenchyma, while parasite-associated products may promote hepatocyte dysfunction through oxidative stress, metabolic disturbance, programmed cell death, and immune dysregulation. These processes can occur together with organelle damage, disruption of hepatocyte integrity, and progressive loss of normal liver architecture. Thus, hepatic CE is likely to reflect the combined effects of mechanical injury and persistent host-parasite molecular interactions.

Studies showed that largely focused on single time points or individual omics layers, limiting the ability to resolve the temporal evolution of host responses during chronic *E. granulosus* infection[11,12]. Available evidence indicates that antiparasitic immunity changes over time, with early cellular inflammatory responses gradually giving way to a more regulatory or Th2-skewed immune environment[13]. Parasite infection is also associated with progressive fibrosis[14,15],

although the molecular events linking immune modulation to tissue remodeling remain incompletely defined. In parallel, metabolic reprogramming has emerged as an important component of host-pathogen interactions[16,17], but its temporal characteristics and potential contribution to CE-associated liver injury have not been systematically examined.

In this study, we established a standardized rat model of hepatic E. granulosus infection and integrated multi-omics analyses to characterize hepatic responses. We focused on identifying molecular pathways shared across disease stages and on defining candidate factors associated with immune regulation, metabolic adaptation, and fibrotic remodeling. Candidate genes and proteins were selected for further evaluation. This longitudinal multi-omics framework was designed to provide an integrated view of host responses during chronic parasite infection and to prioritize candidate pathways for subsequent mechanistic investigation.

2 Materials and methods

2.1 Ethics statement

All animal procedures were approved by the Animal Ethics Committee of Xinjiang Agricultural University (approval No. 2022036) and were performed in accordance with the institutional guidelines for the care and use of laboratory animals. Rats were housed under controlled temperature and humidity with a 12 h light/dark cycle and had free access to standard chow and purified water.

2.2 Isolation and in vitro culture of protoscoleces

Sheep livers containing *E. granulosus* cysts were collected from the Hualing slaughterhouse in Urumqi, Xinjiang, China. Cyst fluid was aspirated aseptically into sterile 50-mL centrifuge tubes and allowed to sediment naturally. After removal of the supernatant, protoscoleces were washed repeatedly with phosphate-buffered saline (PBS) containing penicillin and streptomycin to remove tissue debris. The isolated protoscoleces were maintained in RPMI-1640 medium supplemented with 10% fetal bovine serum (FBS) as described previously.

2.3. Establishment of the rat *E. granulosus* infection model

Sprague-Dawley rats of both sexes (100 ± 10 g) were obtained from the Laboratory Animal Center of Xinjiang Medical University and acclimatized for 1 week before experimentation. Rats were anesthetized, the abdominal cavity was opened surgically, and the liver was exposed. A 0.5-mL protoscolex suspension (20,000 protoscoleces/mL) was injected approximately 1 cm into the right hepatic lobe using a 1-mL syringe inserted at an angle of approximately 45°. After injection, the puncture site was compressed with a sterile dry cotton swab to achieve hemostasis. Procaine penicillin in oil (0.5 mL) was then administered intraperitoneally, the abdominal wall and skin were closed in layers, and the animals were allowed to recover from anesthesia.

2.4 Histopathological analysis

Rat liver tissues were collected and fixed in 4% paraformaldehyde, dehydrated, paraffin embedded, sectioned, deparaffinized, and rehydrated. Sections were stained with hematoxylin and eosin (H&E), mounted, and examined by light microscopy for histopathological changes.

2.5 Transcriptome sequencing and analysis

Total RNA was extracted from liver tissue, and samples passing quality assessment were used to construct strand-specific libraries. Libraries were sequenced on the Illumina NovaSeq 6000 platform to generate 150-bp paired-end reads. After quality control, alignment, and quantification, differentially expressed genes (DEGs) were identified using DESeq2 with |log2 fold change| > 1 and adjusted $P < 0.05$. Gene Ontology (GO) and Kyoto Encyclopedia of Genes and Genomes (KEGG) enrichment analyses were performed using clusterProfiler, with adjusted $P < 0.05$ considered significant.

2.6 Proteomic analysis

Total protein was extracted from liver tissue surrounding the cysts and quantified using the bicinchoninic acid (BCA) assay. Proteins were digested using a filter-aided sample preparation (FASP) workflow, and peptides were fractionated by high-pH reversed-phase chromatography. Data-dependent acquisition (DDA) was used for library generation and data-independent acquisition (DIA) for quantitative analysis[18,19]. Protein identification and quantification were performed using Proteome Discoverer and Skyline, followed by functional annotation against multiple databases.

2.7 Quantitative real-time PCR

Total RNA was extracted from liver tissue using TRIzol reagent and reverse-transcribed into cDNA. Quantitative real-time PCR was performed using SYBR Green chemistry, with GAPDH as the internal reference gene. Relative gene expression was calculated using the 2^-ΔΔCq method.

2.8 Western blotting

Total protein was extracted and quantified, separated by SDS-PAGE, and transferred to membranes. After blocking, membranes were incubated with the indicated primary antibodies followed by the appropriate secondary antibodies, and immunoreactive bands were visualized using chemiluminescence.

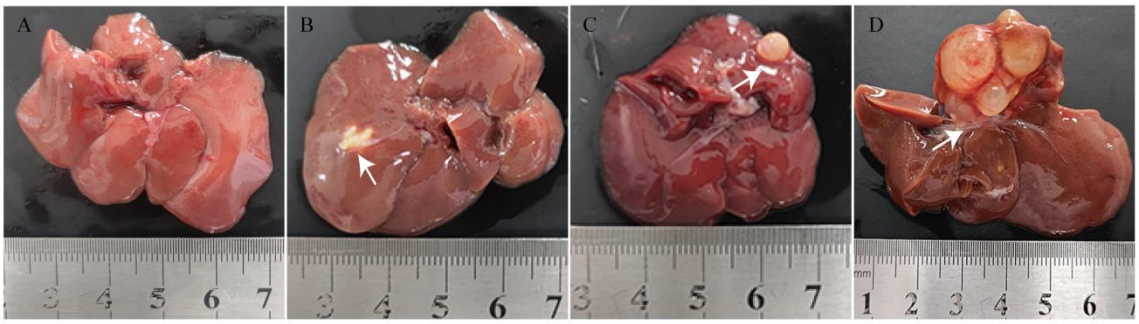
2.9 Statistical analysis

Statistical analyses and graph generation were performed using GraphPad Prism 9.5.0. Depending on the experimental design, differences between two groups were assessed using a two-tailed Student's t-test, whereas comparisons among multiple groups were performed using one-way analysis of variance (ANOVA). Data are presented as the mean ± standard deviation (SD). $P < 0.05$ was considered statistically significant; $*P < 0.05$, $**P < 0.01$, ns, not significant.

3 Results

3.1 Gross morphological changes in hepatic cysts during *E. granulosus* infection

To investigate the progression of hepatic lesions induced by *E. granulosus*, we established a standardized rat model of hepatic *E. granulosus* infection and performed histopathological examination. The results revealed that *E. granulosus* infection produced progressive gross pathological changes in the liver. At 1 month after infection, gray-white nodular cyst-like lesions were visible and were accompanied by extensive hepatocyte necrosis, early fibrous wall formation, and inflammatory cell infiltration in the surrounding tissue(Fig.1 B). By 3 months, the cysts had enlarged, fibrous tissue extended into the adjacent parenchyma, and the hepatic lobular architecture became increasingly disorganized(Fig.1 C). At 6 months, multiple translucent cysts were present, with thinner cyst walls and evidence of neovascularization(Fig.1 D). The surrounding fibrous tissue contained abundant fibroblast-like cells and lymphocytic infiltrates, together with more pronounced fibrosis.

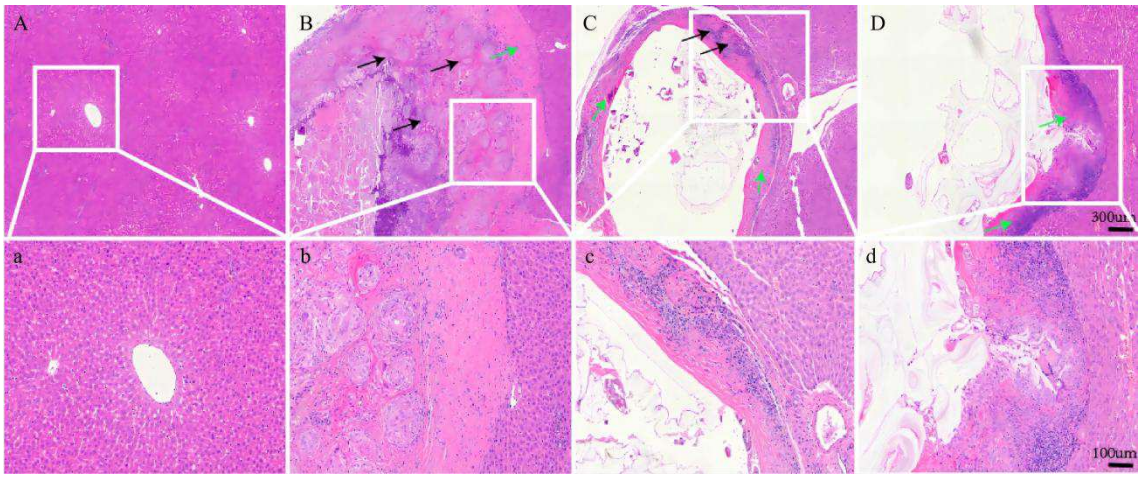


A: Uninfected control rat liver; B: Rat liver at 1 month after *E. granulosus* infection; C: Rat liver at 3 months after *E. granulosus* infection; D: Rat liver at 6 months after *E. granulosus* infection.

Fig.1 Morphological Changes in Rat Liver at Different Time Points After *E. granulosus* Infection

3.2 Histopathological evolution of liver injury during infection

To characterize the histopathological progression of hepatic *E. granulosus* infection, liver tissues from the established rat model were subjected to histopathological examination. The results revealed that at 1 month, limited inflammatory infiltration and early granuloma formation were observed around the lesions, while the hepatic architecture remained relatively preserved despite local mechanical compression(Fig.2 B). At 3 months, granulomatous inflammation and hepatocyte necrosis became more prominent and were accompanied by increasing fibrous tissue proliferation(Fig.2 C). By 6 months, dense fibrous cyst walls with extensive collagen deposition and hyaline-like changes were evident, together with marked disruption and atrophy of adjacent hepatic lobules(Fig.2 D). These observations indicate progressive remodeling of the local hepatic microenvironment as infection became chronic.



A: Uninfected control rat liver; B: Rat liver at 1 month after *E. granulosus* infection; C: Rat liver at 3 months after *E. granulosus* infection; D: Rat liver at 6 months after *E. granulosus* infection. Lowercase letters represent magnified images of local tissue.

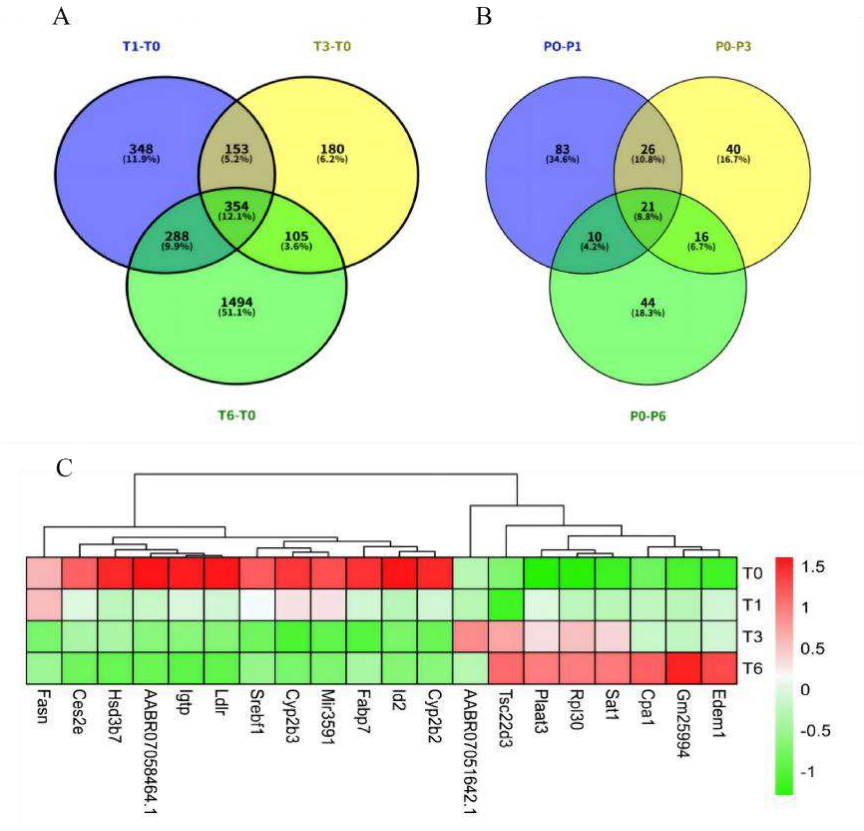
Fig.2 Histological Changes in Rat Liver at Different Time Points After *E. granulosus* Infection(H.E)

3.3 Identification and functional annotation of DEGs and proteins across infection stages

To characterize the host molecular response to hepatic *E. granulosus* infection, we performed integrated transcriptomic and proteomic analyses. The results revealed that transcriptomic analysis identified 348, 180, and 1,494 DEGs at 1, 3, and 6 months, respectively, relative to the control group. A total of 153 genes differed between the 3 months and 1 month groups, whereas 105 genes differed between the 6 months and 3months groups. Across the three infection stages, 354 genes were common to the differential expression datasets(Fig.3 A).

Proteomic analysis likewise identified stage-dependent changes in protein abundance. Relative to controls, 348, 180, and 1,494 differentially expressed proteins were reported at 1, 3, and 6 months, respectively. A total of 153 proteins differed between 3 and 1 months. In addition, 105 differentially expressed features were identified between 6 and 3 months, and 354 were shared across infection stages(Fig.3 B).

Integration of the transcriptomic and proteomic datasets identified 20 genes showing coordinated changes at the mRNA and protein levels. Six were associated with metabolic regulation (Sqor, Pdk4, Cpt1a, Hmgcr, Akr1b7, and Gsta2), encompassing energy metabolism, cholesterol biosynthesis, oxidative-stress responses, and detoxification. Three genes (Cdkn1a, Ccnd1, and Bcl2l11) were related to cell-cycle control and apoptosis. Five genes (Stat1, Irf7, Isg15, Cxcl10, and Mmp8) were associated with immune and inflammatory responses, including interferon signaling and chemokine-mediated cell recruitment. Col4a5, Adamts7, and Spink11 were linked to extracellular-matrix organization and tissue remodeling, whereas Dbh, Syt12, and Esr1 were associated with signaling and gene regulation(Fig.3 C). Together, these overlapping molecules highlighted coordinated alterations in metabolic, immune, and tissue-remodeling processes during infection.

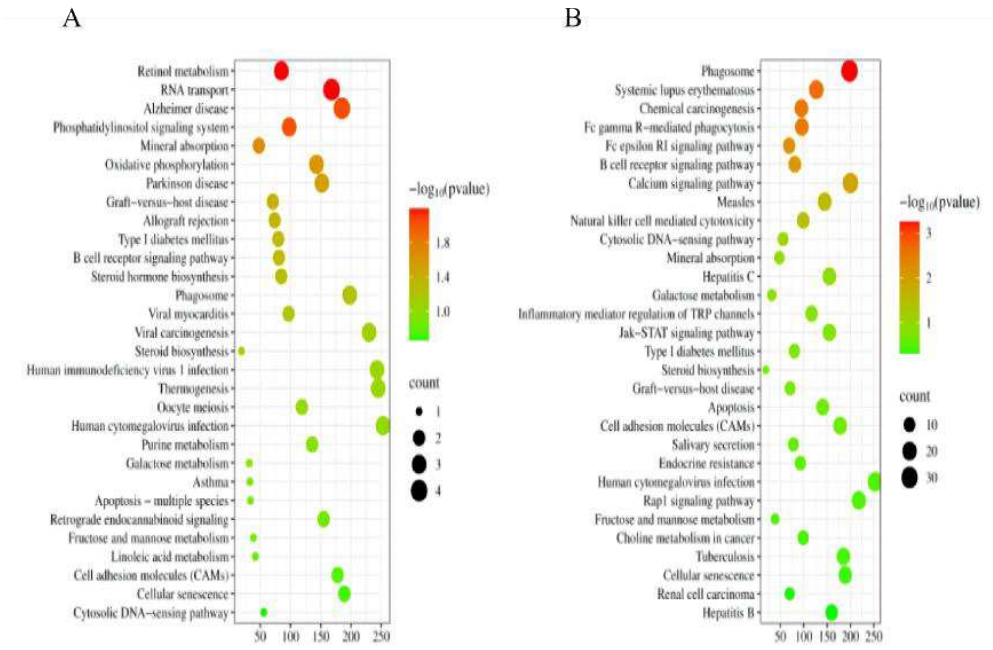


A: Transcriptomic Analyses of DEGs; B: Proteomic Analyses of Differentially Expressed Proteins; C: Statistics of Differentially Expressed Proteins with Concordant Expression Trends Between the Transcriptome and Proteome.

Fig.3 Transcriptomic and Proteomic Analyses of DEGs and Proteins in Rat Liver at Different Time Points After *E. granulosus* Infection

3.4 Shared transcriptomic and proteomic pathways during early infection (1 month)

To characterize the early hepatic host response to *E. granulosus* infection, we performed integrated transcriptomic and proteomic analyses at 1 month after infection. The results revealed that at 1 months after infection, this analysis identified 83 shared KEGG pathways. Among the 30 most significantly enriched pathways, 12 were common to both omics layers. These included immune- and inflammation-related pathways (B-cell receptor signaling, phagosome, cell adhesion molecules, cytosolic DNA-sensing, and graft-versus-host disease), metabolic pathways (mineral absorption, galactose metabolism, fructose and mannose metabolism, and steroid biosynthesis), cellular senescence, and disease-associated pathways including type I diabetes mellitus and human cytomegalovirus infection(Fig.4 and Tab.1). The concurrent enrichment of immune and metabolic pathways indicates that the early stage of infection is characterized by substantial inflammatory signaling together with broad changes in host metabolic regulation. Because pathway enrichment reflects shared molecular signatures rather than direct pathway activity, these associations were interpreted as candidate processes involved in the early host response.



A: KEGG pathway enrichment analysis of DEGs (transcriptome); B: KEGG pathway enrichment analysis of differentially expressed proteins (proteome).

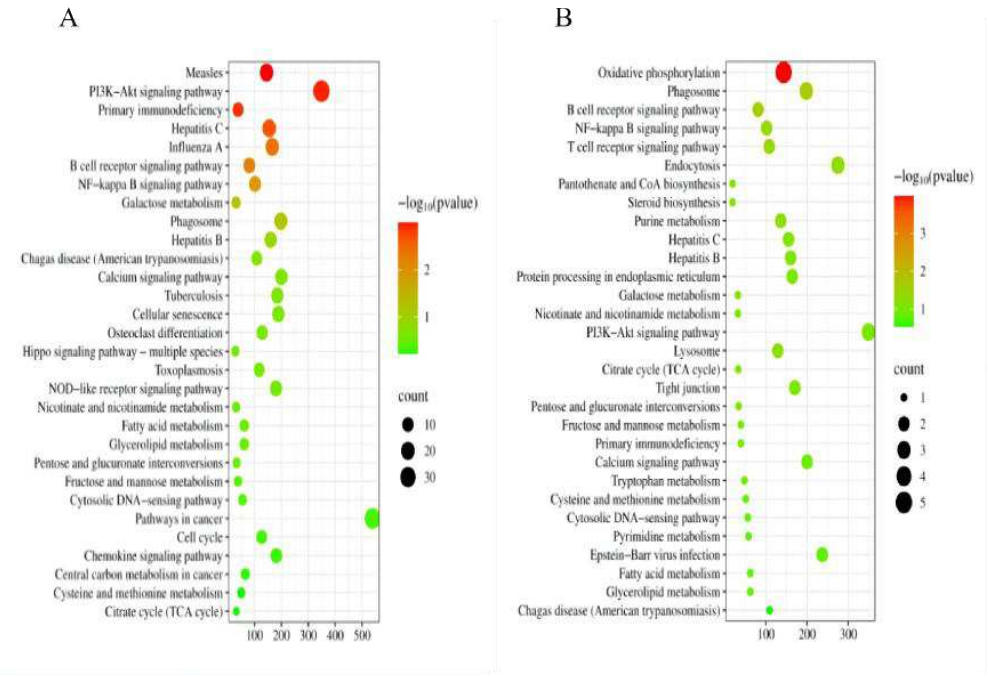
Fig.4 KEGG pathway enrichment analysis of DEGs in Rat Liver at 1 month After *E. granulosus* Infection

Tab.1 Summary of Enriched Signaling Pathways, Functions, and Key Factors in Rat Liver at 1 Month After *E. granulosus* Infection

Shared Signaling Pathways	Functions	Key Factors
B cell receptor signaling pathway	Induces early immunosuppression and Th2 skew, promotes Breg secretion of IL10, suppresses Th1 immunity, and facilitates chronic parasite parasitism.	Stat1, Ccnd1, Bcl10, PI3K, AKT
Phagosome	Inhibits early phagosome maturation and lysosomal fusion, impairs the larvicidal capacity of macrophages, mediates immune paralysis, and supports parasite survival.	Rab5, Rab7, LAMP1, Arp2/3
Cell adhesion molecules (CAMs)	Mediates early intrahepatic migration and adhesion of parasites, and initiates local tissue injury.	α5β1, ICAM-1, VCAM-1, β-catenin
Cytosolic DNA-sensing pathway	Recognizes parasite DNA at the early stage and initiates mild innate immunity to avoid excessive inflammatory injury.	Irf7, Isg15, Cxcl10, cGAS, STING, TBK1
Graft-versus-host disease	Triggers graft-versus-host-like reactions and induces acute hepatic inflammatory injury.	MHC-I/II, TNF-α, IFN-γ, Fas/FasL
Mineral absorption	Deprives calcium, iron and zinc from the host at the early stage, reduces host immune activity, and disturbs calcium signaling homeostasis.	IRP, TfR, CaM, SLC30A8
Galactose metabolism	Hijacks host galactose for parasite glycolysis at the early stage, triggers hepatic metabolic disorder and hepatocyte injury, and sustains parasite proliferation.	Galactokinase (GALK), Hexokinase (HK)
Fructose and mannose metabolism	Enhances carbohydrate scavenging at the early stage to meet the energy demand for rapid parasite proliferation.	Pdk4, Fructokinase (KHK), Hexokinase (HK)
Steroid biosynthesis	Activates cholesterol synthesis at the early stage to supply raw materials for parasite structural formation; causes host lipid accumulation, and high Hmgcr expression promotes fibrosis and parasitism.	Hmgcr, Cyp51, Dhcr7, Sqle, Ldlr
Cellular senescence	Induces hepatocyte senescence instead of apoptosis at the early stage to guarantee nutrient supply for parasites.	Cdkn1a, Ccnd1, p53, IL-6, Mmp3
Type I diabetes mellitus	Induces metabolic disorder via antigen mimicry at the early stage and aggravates the tendency of hepatic injury.	Fas/FasL, CHOP, IRE1α, INS, IRS2
Human cytomegalovirus infection	Mimics viral immune evasion at the early stage, preliminarily inhibits antigen presentation, and benefits parasitism.	MHC-I, UL18, pp65, IE1/2, US2/US11, PD-L1

3.5 Shared transcriptomic and proteomic pathways during intermediate infection (3 months)

To characterize the host molecular responses during hepatic *E. granulosus* infection and identify pathways associated with disease progression, we performed integrated transcriptomic and proteomic analysis. The results revealed that at 3 months after infection, this analysis identified 56 shared KEGG pathways, 18 of which were represented among the 30 most significantly enriched pathways. The shared pathways included immune and inflammatory signaling (phagosome, B-cell receptor signaling, NF-κB signaling, and cytosolic DNA-sensing), metabolic processes (galactose metabolism, fructose and mannose metabolism, the citrate cycle, fatty acid metabolism, and nicotinate and nicotinamide metabolism), chronic infection-associated signatures (hepatitis B, hepatitis C, and Chagas disease), and signaling pathways including PI3K-Akt and calcium signaling(Fig.5 and Tab.2). Additional shared pathways included primary immunodeficiency, pentose and glucuronate interconversions, glycerolipid metabolism, and cysteine and methionine metabolism. Compared with the early stage, the broader representation of inflammatory, metabolic, and tissue-remodeling pathways at 3 months was consistent with a transition toward a more persistent inflammatory and fibrotic state.



A: KEGG pathway enrichment analysis of DEGs (transcriptome); B: KEGG pathway enrichment analysis of differentially expressed proteins (proteome).

Fig.5 KEGG pathway enrichment analysis of DEGs in Rat Liver at 3 months After *E. granulosus* Infection

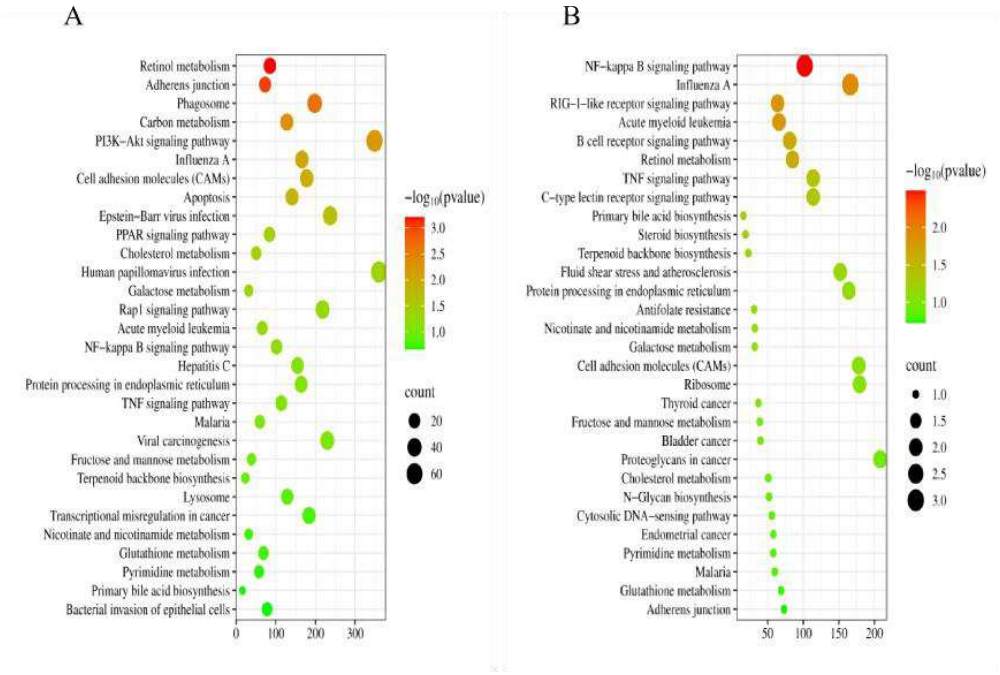
Tab.2 Summary of Enriched Signaling Pathways, Functions, and Key Factors in Rat Liver at 3 Months After *E. granulosus* Infection

Shared Signaling Pathways	Biological interpretation	Key Factors
B cell receptor signaling pathway	Associated with continued B-cell signaling and potential regulatory immune remodeling during intermediate infection.	Stat1, Ccnd1, Bcl10, PI3K, AKT
Phagosome	Suggests persistent alteration of phagosome-related functions during intermediate infection.	Rab5, Rab7, LAMP1, Arp2/3

NF-κB signaling pathway	Associated with sustained inflammatory signaling during intermediate infection.	NF-κB, p65, MyD88, TNF-α, IL-6
Galactose metabolism	Indicates persistent remodeling of galactose metabolism during intermediate infection.	Galactokinase (GALK), Hexokinase (HK)
Cytosolic DNA-sensing pathway	Associated with continued nucleic-acid-sensing and interferon-related signaling during intermediate infection.	Irf7, Isg15, Cxcl10, cGAS, STING, TBK1
Primary immunodeficiency	Represents an immune-associated signature overlapping with the primary immunodeficiency pathway.	CD3, CD4, CD8, IL-2R, JAK3, STAT5
Hepatitis C	Represents a chronic-inflammation signature overlapping with the hepatitis C pathway.	TNF-α, TGF-β1, Smad3, MMP9
Hepatitis B	Represents an immune-regulatory signature overlapping with the hepatitis B pathway.	PD-L1, IL-10, TGF-β1, NF-κB
Chagas disease (American trypanosomiasis)	Represents a chronic inflammatory signature overlapping with the Chagas disease pathway.	TLR2, TLR4, NF-κB, TNF-α, IL-10, TGF-β1
Calcium signaling pathway	Suggests altered calcium-dependent signaling during intermediate infection.	IP3R, Calmodulin (CaM), CaMKII
Fatty acid metabolism	Indicates remodeling of fatty-acid metabolism during intermediate infection.	FASN, ACSL1, CPT1A, HMGCR
Nicotinate and nicotinamide metabolism	Suggests altered nicotinate and nicotinamide metabolism and cellular redox-energy balance during intermediate infection.	NAMPT, NAD+, PARP, SIRT1, NRK1, PNP
Pentose and glucuronate interconversions	Indicates altered pentose and glucuronate interconversions, with potential effects on carbon partitioning and detoxification.	UGT1A, G6PD, RPIA, TKTL1, ALDOA, PKM2
Fructose and mannose metabolism	Indicates persistent remodeling of fructose and mannose metabolism during intermediate infection.	Pdk4, Fructokinase (KHK), Hexokinase (HK)
Cysteine and methionine metabolism	Indicates altered sulfur-amino-acid metabolism and redox homeostasis during intermediate infection.	CBS, CSE, MAT1A, AHCY, GST, GPX1
Citrate cycle (TCA cycle)	Suggests remodeling of TCA-cycle-related mitochondrial metabolism during intermediate infection.	IDH2, SDHB, FH, MDH1, PDHA1
PI3K-Akt signaling pathway	Associated with PI3K-Akt signaling during intermediate-stage tissue and immune remodeling.	PI3K, Akt, mTOR, PTEN, Bad, Cyclin D1

3.6 Shared transcriptomic and proteomic pathways during late infection (6 months)

To characterize the molecular landscape of late-stage hepatic *E. granulosus* infection and to identify pathways shared across disease stages, we performed KEGG enrichment analysis on integrated transcriptomic and proteomic data. The results revealed that at 6 months after infection, this analysis identified 55 shared KEGG pathways, including 17 pathways among the 30 most significantly enriched terms. These comprised immune and inflammatory pathways (NF-κB signaling, phagosome, B-cell receptor signaling, TNF signaling, C-type lectin receptor signaling, and cytosolic DNA-sensing), metabolic pathways (retinol metabolism, galactose metabolism, fructose and mannose metabolism, nicotinate and nicotinamide metabolism, cholesterol metabolism, terpenoid backbone biosynthesis, and glutathione metabolism), cell adhesion and adherens junction pathways, PI3K-Akt signaling, and an influenza A-associated gene signature(Fig.6 and Tab.3). Together with the histological evidence of advanced fibrosis, these enrichment patterns suggest that late-stage infection is accompanied by sustained inflammatory signaling, extensive metabolic adaptation, and pronounced tissue remodeling. Disease-name KEGG terms were interpreted as shared molecular signatures and not as evidence of the corresponding diseases.



A: KEGG pathway enrichment analysis of DEGs (transcriptome); B: KEGG pathway enrichment analysis of differentially expressed proteins (proteome).

Fig.6 KEGG pathway enrichment analysis of DEGs in Rat Liver at 6 months After *E. granulosus* Infection

Tab.3 Summary of Enriched Signaling Pathways, Functions, and Key Factors in Rat Liver at 6 Months After *E. granulosus* Infection

Pathway Name	Biological interpretation	Key Factors
NF-κB signaling pathway	Associated with persistent inflammatory signaling and fibrotic remodeling during late infection.	NF-κB, p65, MyD88, TNF-α, IL-6
Phagosome	Suggests persistent alteration of phagosome-related functions during late infection.	Rab5, Rab7, LAMP1, Arp2/3
B cell receptor signaling pathway	Associated with continued B-cell signaling and regulatory immune remodeling during late infection.	Stat1, Ccnd1, Bcl10, PI3K, AKT
TNF signaling pathway	Associated with inflammatory and cell-death signaling during late infection.	TNF-α, TNFR1, Caspase-3
Cytosolic DNA-sensing pathway	Associated with persistent innate nucleic-acid-sensing pathways during late infection.	Irf7, Isg15, Cxcl10, cGAS, STING, TBK1
Retinol metabolism	Indicates altered retinol metabolism during late infection, with potential relevance to hepatic repair and fibrosis.	RPE65, ALDH1A1, Retinoic acid
Galactose metabolism	Indicates persistent remodeling of galactose metabolism during late infection.	Galactokinase (GALK), Hexokinase (HK)
Fructose and mannose metabolism	Indicates persistent remodeling of fructose and mannose metabolism during late infection.	Pdk4, Fructokinase (KHK), Hexokinase (HK)
Nicotinate and nicotinamide metabolism	Suggests altered nicotinate/nicotinamide metabolism and cellular redox-energy balance during late infection.	NAMPT, NAD+, PARP, SIRT1, NRK1, PNP
Cholesterol metabolism	Indicates remodeling of cholesterol metabolism during late infection.	HMGCR, CYP51, LDLR
Terpenoid backbone biosynthesis	Suggests altered terpenoid-backbone biosynthesis during late infection.	HMGR, FPPS, GGPPS
Glutathione metabolism	Indicates altered glutathione metabolism and redox homeostasis during late infection.	GCL, GSS, GPx, GR
Cell adhesion molecules (CAMs)	Associated with cell adhesion and fibrotic tissue remodeling during late infection.	α5β1, ICAM-1, VCAM-1, β-catenin
Adherens junction	Suggests remodeling of adherens-junction-associated tissue architecture during late infection.	E-cadherin, β-catenin, α-catenin

PI3K-Akt signaling pathway	Associated with PI3K-Akt signaling during late-stage tissue and immune remodeling.	PI3K, Akt, mTOR, PTEN, Bad, Cyclin D1
Influenza A	Represents an inflammatory gene signature overlapping with the influenza A pathway.	IFN-α/β, IRF3, NF-κB, TNF-α

3.7 Core pathways shared throughout the course of *E. granulosus* infection

To identify biological pathways that are consistently represented throughout chronic hepatic *E. granulosus* infection, we compared the integrated transcriptomic and proteomic datasets across 1, 3, and 6 months after infection. The results revealed that six pathways were consistently represented throughout infection: B-cell receptor signaling, phagosome, cytosolic DNA-sensing, cell adhesion molecules, galactose metabolism, and fructose and mannose metabolism(Tab.4). These pathways collectively encompass immune regulation, phagocytic function, cell-matrix interactions, and carbohydrate metabolism. Their persistent representation across all three time points suggests that these biological processes may constitute a common molecular framework of the host response during the establishment and maintenance of chronic *E. granulosus* infection.

Tab.4 Summary of Enriched Signaling Pathways, Functions, and Key Factors in Rat Liver at 1, 3, and 6 Months After *E. granulosus* Infection

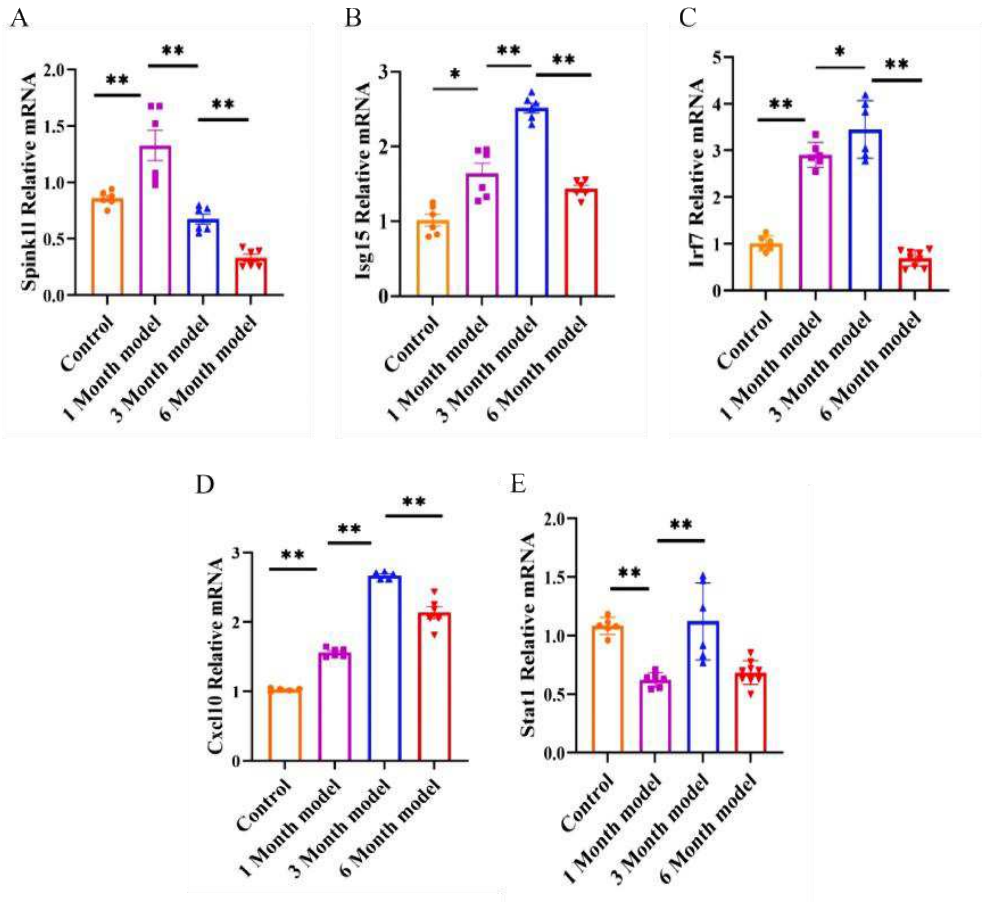
Shared Signaling Pathways	Biological interpretation	Key Factors
B cell receptor signaling pathway	Persistently enriched across infection and associated with B-cell-mediated immune regulation.	Stat1, Ccnd1, Bcl10, PI3K, AKT
Phagosome	Persistently enriched across infection and associated with phagosome-related immune functions.	Rab5, Rab7, LAMP1, Arp2/3
Cell adhesion molecules (CAMs)	Persistently enriched across infection and associated with cell adhesion and tissue remodeling.	α5β1, ICAM-1, VCAM-1, β-catenin
Cytosolic DNA-sensing pathway	Persistently enriched across infection and associated with innate nucleic-acid sensing and inflammatory regulation.	Irf7, Isg15, Cxcl10, cGAS, STING, TBK1
Galactose metabolism	Persistently enriched across infection and indicative of altered galactose metabolism.	Galactokinase (GALK), Hexokinase (HK)
Fructose and mannose metabolism	Persistently enriched across infection and indicative of altered fructose and mannose metabolism.	Pdk4, Fructokinase (KHK), Hexokinase (HK)

3.8 Transcriptional validation of selected DEGs

3.8.1 Dynamic changes in immune-response genes across infection stages

To determine how innate immunity and inflammation are regulated during hepatic *E. granulosus* infection, we analyzed the expression of immune-related genes across infection stages. The results revealed that from 1 to 3 months after infection, Spink1 was elevated at 1 month but decreased at 3 months and 6 months(Fig.7 A), whereas Isg15, Irf7, and Cxcl10 were markedly increased, and reached their highest levels at 3 months(Fig.7 B, Fig.7 C, and Fig.7 D), consistent with pronounced interferon-associated signaling and inflammatory cell recruitment during the intermediate stage. Stat1 showed a modestly different pattern, with an initial decrease followed by partial recovery(Fig.7 E). At 6 months, most immune-related transcripts declined; Spink1, Irf7, and Stat1 fell to or below control levels, whereas Isg15 and Cxcl10 were also reduced relative to the earlier stages. This temporal pattern is consistent with attenuation or

redistribution of the early inflammatory response as infection becomes chronic, although functional immune tolerance or exhaustion was not directly assessed.

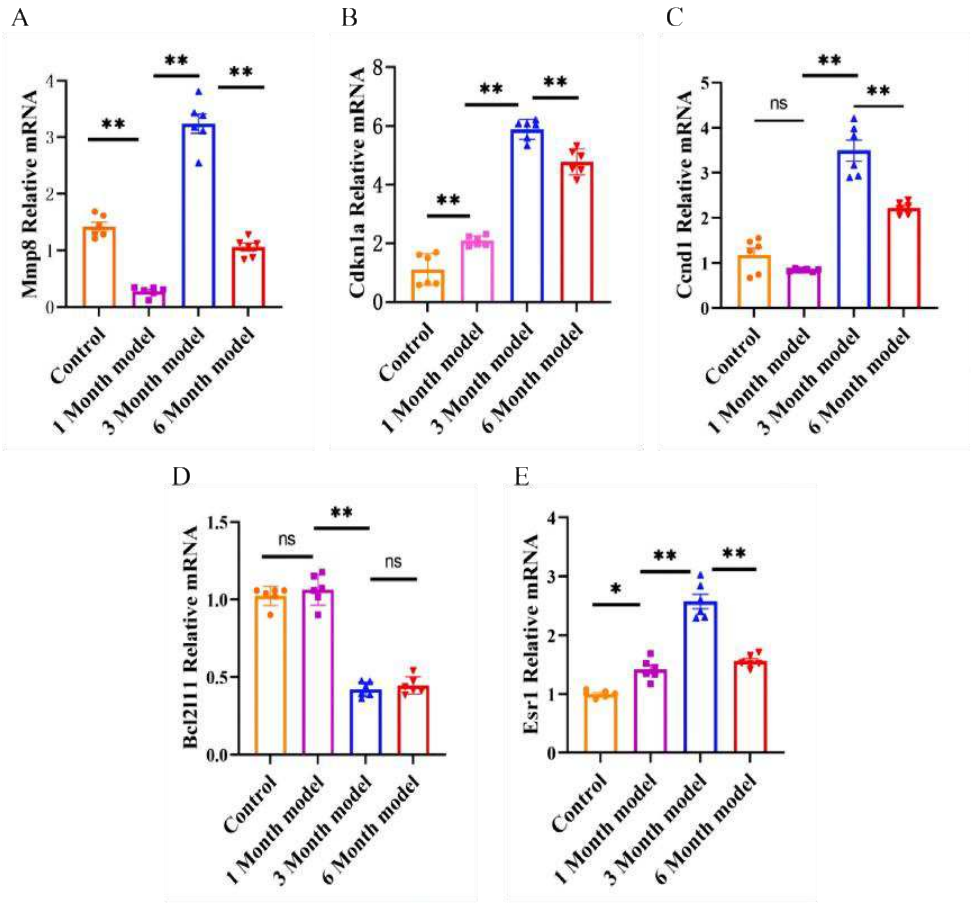


A: Relative mRNA expression of Spink11; B: Relative mRNA expression of Isg15; C: Relative mRNA expression of Irf7; D: Relative mRNA expression of Cxcl10; E: Relative mRNA expression of Stat1.

Fig.7 Relative mRNA Expression Levels of Spink11, Isg15, Irf7, Cxcl10, and Stat1 Key Factors in Rat Liver at 1, 3, and 6 Months after *E. granulosus* infection

3.8.2 Stage-dependent changes in genes related to cell-cycle control, remodeling, and apoptosis

To investigate the dynamic regulation of cell fate during chronic hepatic *E. granulosus* infection, we examined the expression of genes involved in cell-cycle regulation, tissue remodeling, and apoptosis. The results showed that these genes exhibited pronounced temporal changes, with 3 months representing an important transition point. Mmp8, Cdkn1a, Ccnd1, and Esr1 reached their highest transcript levels at 3 months(Fig.8 A, Fig.8 B, Fig.8 C, and Fig.8 E), indicating concurrent activation of tissue remodeling, cell-cycle regulatory programs, and compensatory proliferative responses. At 6 months, Cdkn1a and Ccnd1 remained elevated, whereas the pro-apoptotic gene Bcl2l11 was specifically down-regulated starting at 3 months and remained at a low level at 6 months(Fig.8 D). These findings suggest persistent dysregulation of cell fate during chronic liver injury and may reflect an adaptive balance between cell-cycle arrest, proliferation, and cell survival.



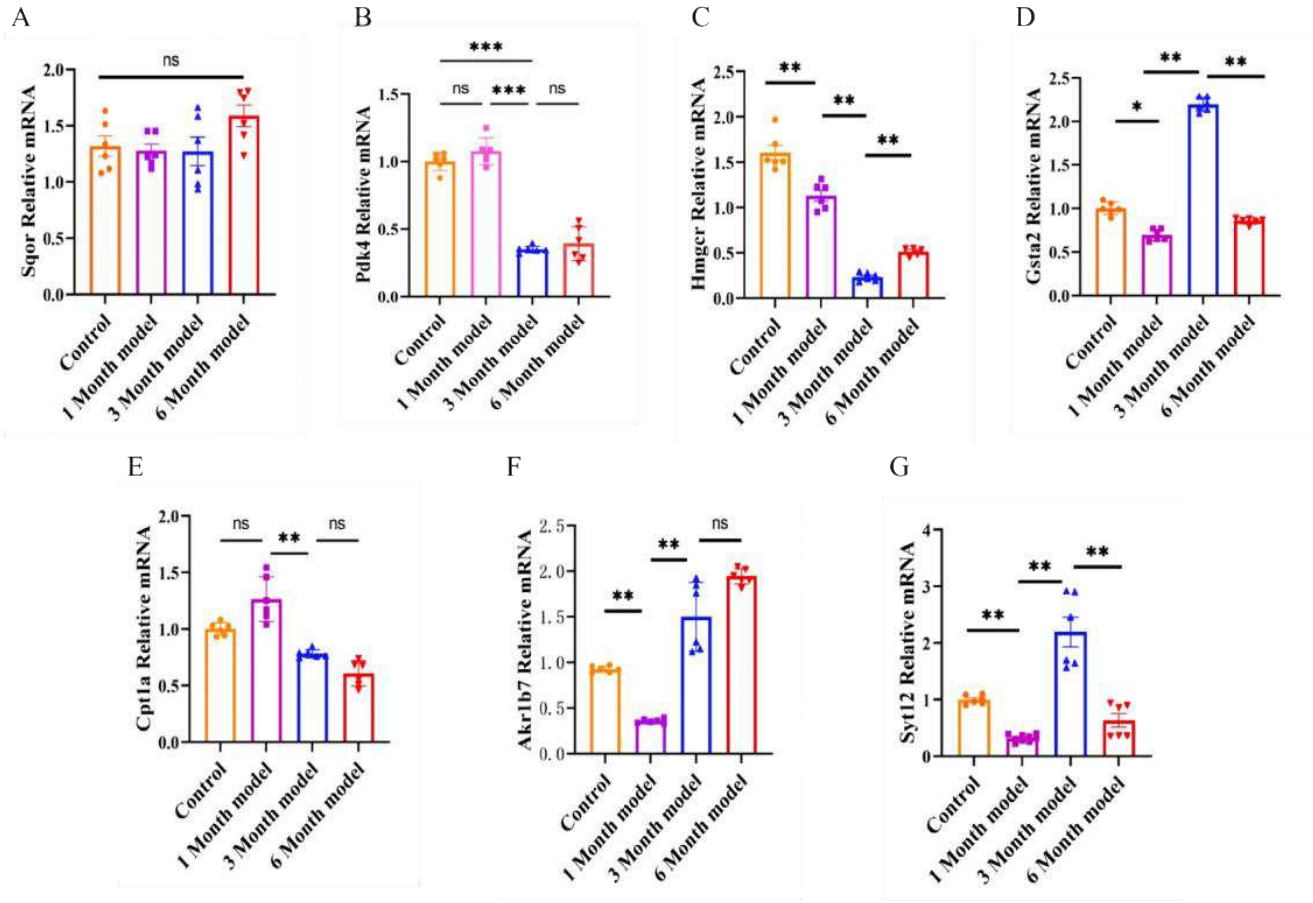
A: Relative mRNA expression of Mmp8; B: Relative mRNA expression of Cdkn1a; C: Relative mRNA expression of Ccnd1; D: Relative mRNA expression of Bcl2l11; E: Relative mRNA expression of Esr1.

Fig.8 Relative mRNA Expression Levels of Mmp8, Cdkn1a, Ccnd1, Bcl2l11, and Esr1 Key Factors in Rat Liver at 1, 3, and 6 Months after *E. granulosus* infection

3.8.3 Metabolic gene expression indicates sustained impairment of hepatic biosynthetic and detoxification functions

To determine how chronic *E. granulosus* infection affects hepatic biosynthetic and detoxification capacity, we analyzed the expression of genes involved in cholesterol synthesis, xenobiotic and bile-acid metabolism, and antioxidant defense. The results showed that infection was accompanied by marked changes in genes involved in hepatic biosynthesis and detoxification. Sqor expression showed no significant changes across the infection period(Fig.9 A). Pdk4 expression was significantly decreased at 3 months and remained low at 6 months(Fig.9 B), and Hmgcr, a rate-limiting enzyme in cholesterol synthesis was reduced across the infection period(Fig.9 C). In contrast, genes associated with detoxification and antioxidant defense showed stage-specific responses: Gsta2 increased prominently at 3 months and then decreased at 6 months(Fig.9 D), whereas Akr1b7 was decreased at 1 month and elevated at 3 and 6 months(Fig.9 F). Additionally, Cpt1a expression was elevated at 3 months(Fig.9 E), and Syt12 expression was decreased at 1 month, increased at 3 months, and then decreased at 6 months(Fig.9 G). Overall, these transcriptional patterns indicate that chronic infection is accompanied by both impaired hepatic metabolic capacity and

compensatory stress responses.

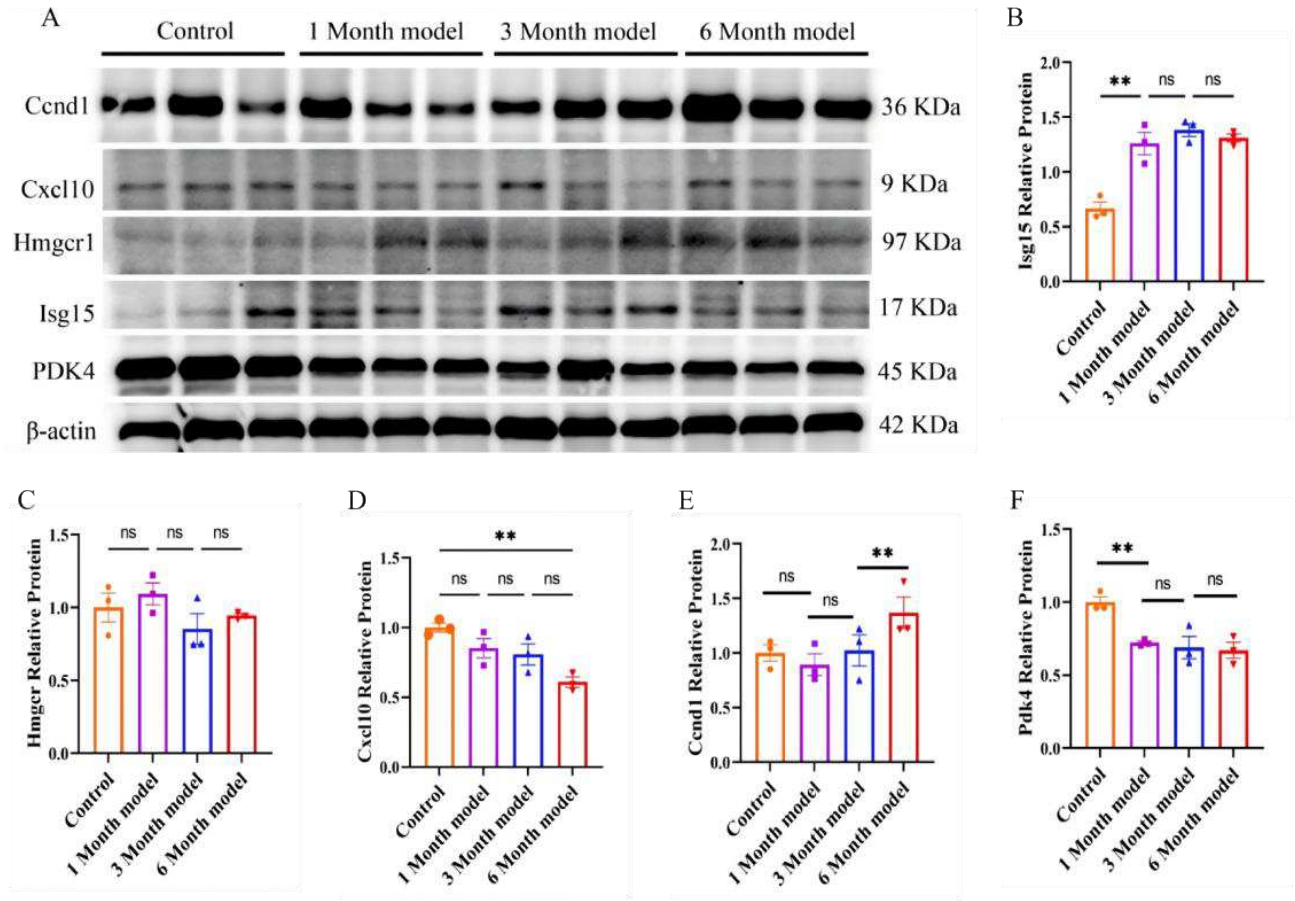


A: Relative mRNA expression of Mmp8; B: Relative mRNA expression of Cdkn1a; C: Relative mRNA expression of Ccnd1; D: Relative mRNA expression of Bcl2l11; E: Relative mRNA expression of Esr1.

Fig.9 Relative mRNA Expression Levels of Spor, Pdk4, Hinger, Gsta2, Cpt1a, Akr1b7, and Syt12 Key Factors in Rat Liver at 1, 3, and 6 Months after *E. granulosus* infection

3.9 Protein-level validation of selected pathways

To validate the candidate proteins identified by integrated multi-omics analyses and to define their stage-dependent alterations during *E. granulosus* infection, we performed Western blotting on selected proteins in liver tissues from infected rats. The results showed that the levels of candidate proteins exhibited distinct time-dependent changes: Ccnd1 protein abundance increased progressively and was highest at 6 months(Fig.10 E). Isg15 was barely detectable in control liver but was markedly increased at all infection time points(Fig.10 B). Hmgcr showed a moderate increase during the early and intermediate stages(Fig.10 C), whereas PDK4 progressively decreased as infection advanced(Fig.10 F). In contrast, Cxcl10 protein abundance did not show an obvious difference among groups(Fig.10 D). These results confirm that proteins involved in cell-cycle regulation, cholesterol metabolism, innate immune responses, and glucose metabolism are altered during infection, while also illustrating that transcript-level changes are not uniformly reflected at the protein level.



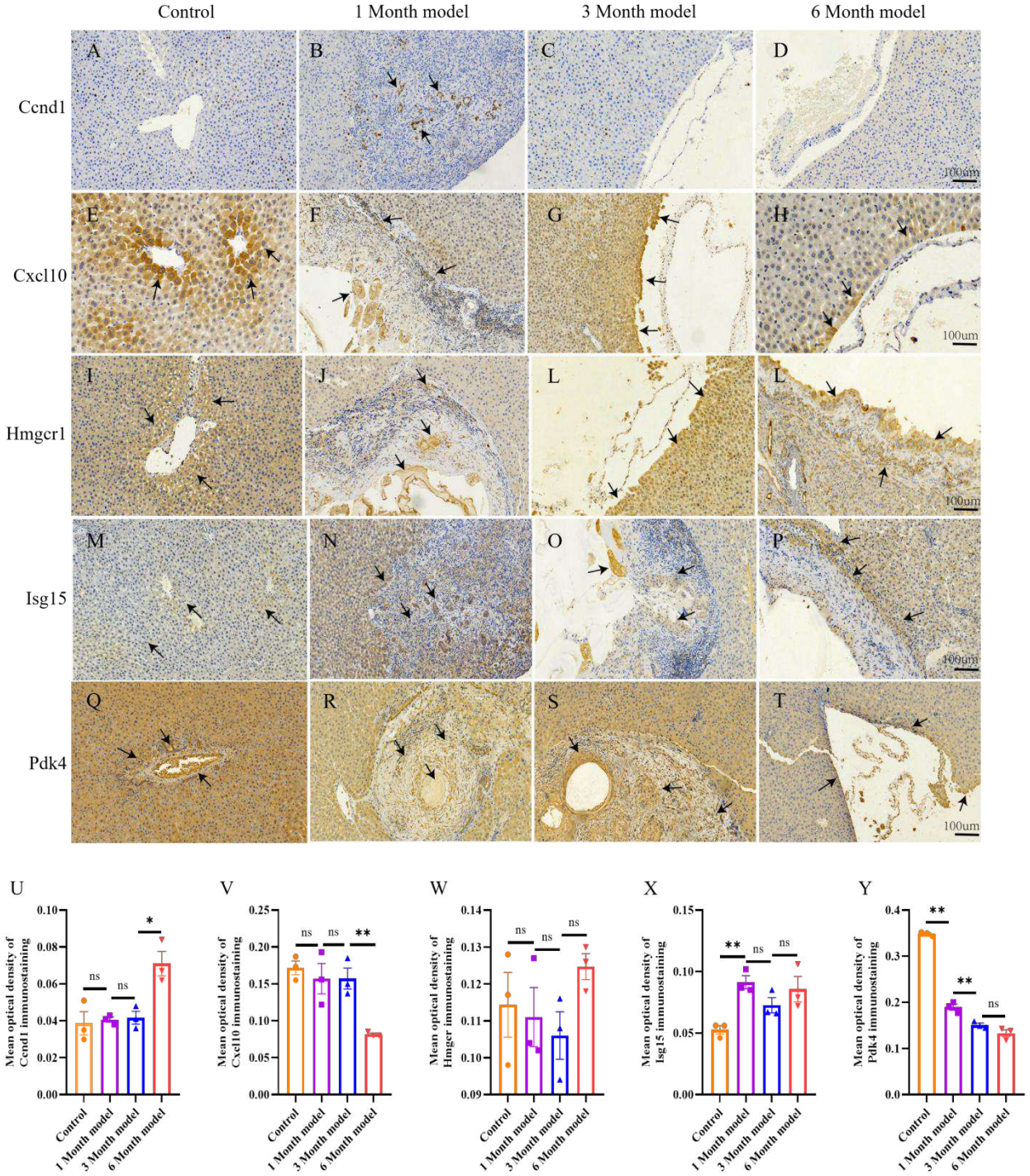
A: Western blot analysis Ccnd1, Cxcl10, Hmgcr1, Isg15, and PDK4 key protein expression in rat liver at 1, 3, and 6 months after *E. granulosus* infection; B: Quantification of relative protein levels of Isg15; C: Quantification of relative protein levels of Hmgcr1; D: Quantification of relative protein levels of Cxcl10; E: Quantification of relative protein levels of Ccnd1; F: Quantification of relative protein levels of PDK4.

Fig.10 Western Blot Analysis and Quantification of Ccnd1, Cxcl10, Hmgcr1, Isg15, and PDK4 Key Protein Expression in Rat Liver at 1, 3, and 6 Months after *E. granulosus* infection

3.10 Spatial localization of selected proteins in liver tissue

To validate the candidate proteins identified by integrated multi-omics analyses and to define their stage-dependent alterations during *E. granulosus* infection, we performed immunohistochemistry (IHC) and quantitative optical density analysis on selected proteins in liver tissues from infected rats. The results showed that the levels of candidate proteins exhibited distinct time-dependent changes: Ccnd1 protein abundance was relatively low in the early stages but increased significantly at 6 months (Fig.11 A-D, U). Isg15 was barely detectable in the control liver but was markedly increased at all infection time points, particularly at 1 and 3 months (Fig.11 M-P, X). Hmgcr showed a relatively stable expression during the early and intermediate stages, with a moderate increase at 6 months (Fig.11 I-L, W), whereas Pdk4 progressively decreased as infection advanced, dropping significantly from 1 month onward (Fig.11 Q-T, Y). In contrast, Cxcl10 protein abundance maintained a high baseline in the control group but decreased significantly at 6 months post-infection (Fig.11 E-H, V). These results confirm that proteins involved in cell-cycle regulation, cholesterol metabolism, innate immune responses, and glucose metabolism are altered during infection,

while also illustrating the dynamic, stage-dependent changes of these proteins in the liver microenvironment.



A-T: Immunohistochemistry (IHC) staining was performed to detect the expression of Ccnd1, Cxcl10, Hmgcr1, Isg15, and Pdk4 in the Control group and 1, 3, and 6 month after *E. granulosus* infection; U: Semi-quantitative Analysis of Mean Optical Density for Ccnd1 Immunohistochemistry; V: Semi-quantitative Analysis of Mean Optical Density for Cxcl10 Immunohistochemistry ; W: Semi-quantitative Analysis of Mean Optical Density for Hmgcr1 Immunohistochemistry; X: Semi-quantitative Analysis of Mean Optical Density for Isg15 Immunohistochemistry; Y: Semi-quantitative Analysis of Mean Optical Density for Pdk4 Immunohistochemistry.

Fig.11 Immunohistochemical staining and quantitative analysis of related proteins in model groups in Rat Liver at 1, 3, and 6 Months after *E. granulosus* infection

4 Discussion

By combining longitudinal histopathology with transcriptomic, proteomic, and targeted validation analyses, this study characterized the evolution of hepatic responses to *E. granulosus* infection at 1, 3, and 6 months. The data indicate that chronic infection is accompanied by coordinated changes in immune signaling, cellular remodeling, and host metabolism rather than by a single dominant molecular pathway. Six pathways were shared across all time points, including B-cell receptor signaling, phagosome, cytosolic DNA-sensing, cell adhesion molecules, galactose metabolism, and fructose and mannose metabolism. In parallel, Stat1 and Ccnd1 exhibited distinct temporal and spatial expression patterns that mirrored the transition from inflammatory lesions to mature fibrous encapsulation[20]. These findings provide a longitudinal framework for understanding how host responses evolve during chronic hepatic CE.

Immune regulation was a prominent component of the host response throughout infection[21]. During the early and intermediate stages, increased expression of Irf7, Isg15, and Cxcl10, together with strong Stat1 staining in inflammatory infiltrates[22], was consistent with activation of interferon-associated and innate immune programs. By 6 months, however, several immune-related transcripts declined and Stat1 staining became largely restricted to the fibrous cyst wall. This change suggests that the immune response becomes spatially and quantitatively remodeled as chronic infection is established. Persistent enrichment of B-cell receptor, phagosome, and cytosolic DNA-sensing pathways further supports continued immune engagement[23,24]. Nevertheless, pathway enrichment alone cannot establish Th2 polarization, regulatory B-cell activation, or impaired phagosome maturation[25]; these mechanisms will require direct cellular and functional validation[26].

Metabolic remodeling represented a second major feature of infection. Galactose metabolism and fructose and mannose metabolism were among the pathways consistently represented across the three time points, whereas additional changes involved the citrate cycle, fatty acid metabolism, cholesterol metabolism, nicotinate and nicotinamide metabolism, and glutathione metabolism at later stages[27-29]. At the gene level, sustained suppression of Hmgcr and Sult1a2, together with stage-specific changes in Gsta2 and Akr1b7, indicated altered biosynthetic, detoxification, and antioxidant functions. These observations are compatible with progressive metabolic stress in the infected liver. However, enrichment and expression data do not directly measure metabolic flux[30], and future isotope-tracing or targeted metabolomic studies will be required to determine whether the parasite directly redirects host carbon sources or whether these changes primarily reflect secondary responses to chronic tissue injury.

Progressive tissue remodeling and fibrosis were closely associated with the duration of infection. Histologically, early inflammatory and granulomatous lesions evolved into dense fibrous encapsulation with extensive collagen deposition by 6 months. Ccnd1 expression was particularly informative in this context[31]. Whereas Ccnd1 staining was associated mainly with hepatocytes at earlier stages, strong staining was observed in the fibrous cyst wall and

fibroblast-like cells at the late stage. Together with sustained Cdkn1a and Ccnd1 transcript expression, this pattern suggests continued cell-cycle remodeling within the chronically injured tissue[32]. Because Ccnd1 is a general regulator of proliferation[33,34], its enrichment in fibrotic regions does not by itself demonstrate that it drives fibrosis; functional perturbation studies will be required to define its cell-specific contribution.

Several molecules, including Stat1, Rab5, ICAM-1, GALK, and Pdk4, were represented in more than one enriched pathway or functional category, highlighting potential points of convergence between immune, metabolic, and structural responses[34]. Such highly connected factors may be useful candidates for subsequent mechanistic studies. In particular, integrating their temporal expression with cell-type-specific localization and functional perturbation could help distinguish drivers of disease progression from downstream markers of tissue damage.

This study has several limitations. First, although the rat model reproduced key pathological features of hepatic CE, experimental infection does not fully recapitulate the complexity of natural human disease. Second, the integrated omics analyses identify associations and pathway-level changes but do not establish causality; genetic perturbation, pharmacological inhibition, and cell-specific functional assays will be needed to test the roles of candidate molecules[11]. Third, the sample size was limited, which may reduce statistical power, particularly for network-level analyses. Finally, pathway enrichment based on disease-related KEGG terms should be interpreted as overlap in molecular signatures rather than direct evidence of those diseases or immune states. Future studies combining larger cohorts, targeted metabolic measurements, in vitro validation, and in vivo functional experiments will be important for defining the mechanisms underlying chronic parasite persistence and fibrosis.

5 Conclusions

Integrated longitudinal multi-omics analysis revealed that *E. granulosus* infection is accompanied by progressive remodeling of immune, metabolic, and tissue-remodeling pathways in the rat liver. Six pathways—B-cell receptor signaling, phagosome, cytosolic DNA-sensing, cell adhesion molecules, galactose metabolism, and fructose and mannose metabolism—were consistently represented across 1, 3, and 6 months of infection. These molecular changes occurred in parallel with hepatocyte injury, increasing fibrosis, and dynamic changes in cyst architecture. Stat1 and Ccnd1 showed particularly distinct temporal and spatial expression patterns and therefore represent candidate markers and mechanistic targets for further investigation. Overall, the study provides a systems-level view of the host response during chronic hepatic CE and a basis for future functional studies aimed at identifying host-directed therapeutic strategies.

Supplementary Materials: No additional materials provided.

Acknowledgments: We sincerely thank Chenghui Xu (engineer, Wekemo Tech Group Co., Ltd., Shenzhen, China) for his guidance on data analysis.

Funding: This research was funded by the Key Project of the Natural Science Foundation of Xinjiang Uygur Autonomous Region (2023D01D04); the Open Project of the National Key Laboratory for Diagnosis and Treatment of Severe Zoonotic Infectious Diseases (RCGHCRB202501); and the Project Task Assignment for the Autonomous Region's Modern Livestock and Poultry Breeding Enhancement Plan.

Conflicts of Interest: All authors have no conflict of interest.

Institutional Review Board Statement: All animal experiments were performed in strict accordance with the guidelines for the Care and Use of Laboratory Animals issued by the Chinese Government. The experimental protocol was approved by the Animal Care and Use Committee of Xinjiang Agricultural University (approval No. 2022036; approved on 27 January 2022).

Informed Consent Statement: Not applicable.

Data Availability Statement: The raw sequencing data and datasets generated and analyzed during the current study are available from the corresponding author upon reasonable request.

Materials availability: This study did not generate new unique biological materials.

Code availability: Not applicable.

Author Contributions: S. Z. conceived and designed the study, developed the methodology, acquired research resources. S. Z. and L. L. performed formal data analysis, and drafted, reviewed, and edited the manuscript. L. L., X. M. and J. Z. established the rat infection model and performed the animal experiments. L. L. and W. L. organized, curated, and validated the experimental data. Z. E. performed histological and immunohistochemical analyses. All authors read and approved the final manuscript.

References

[1] Tunger O.(2013) Epidemiology of Cystic Echinococcosis in the World. Turkish Journal of Parasitology,37(1):47-52.https://doi:10.5152/tpd.2013.12.

[2] Kumar A, Hande V.(2026) Shifting Paradigms in Cholangiohydatidosis: Is Endotherapy Transforming from a Bridge to Definitive Monotherapy? Journal of Digestive Endoscopy.2026.https://doi:10.1055/s-0046-1827251.

[3] Kalita JM, Naveenraj P, Jain V*, et al.*(2022) Cystic Echinococcosis of Liver and Spleen Communicating to the Lung: A Rare Case. Journal of laboratory physicians,14(3):351-354.https://doi:10.1055/s-0042-1742416.

[4] Calu V, Enciu O, Toma EA*, et al.*(2024) Complicated Liver Cystic Echinococcosis—A Comprehensive Literature Review and a Tale of Two Extreme Cases. Tomography: A Journal for Imaging Research,10(6).https://doi:10.3390/tomography10060070.

[5] Deeb S, Sayyedahmad D, Sharif Z, *et al.*(2025) Successful management of a rare extensive hepatopulmonary hydatidosis with over 35 cysts: A case report and literature review. International Journal of Surgery Case Reports,134(C):111807-111807.https://doi:10.1016/j.ijscr.2025.111807.

[6] Lloyd J, Koep L, Yu E, *et al.*(2014) Hepatic cystic echinococcosis. Journal of the American Osteopathic Association,114(06).https://doi:10.7556/jaoa.2014.069.

[7] Chuelov SB, Rossina AL.(2023) Cystic echinococcosis. CHILDREN INFECTIONS.https://doi:10.22627/2072-8107-2023-22-1-50-55.

[8] Barreto I, Deibel A, Fehr J, *et al.*(2026) Surgical management of cystic echinococcosis—A 20-year case series and outcome analysis. PLoS neglected tropical diseases,20(4):e0013661-e0013661. https://doi:10.1371/journal.pntd.0013661.

[9] Bakhtiar NM, Mahami-Oskouei M, Ahmadpour E, *et al.*(2010) Current challenges and future prospects in patients with recurrent cystic echinococcosis; an updated mini review. Experimental Parasitology,277(000):6.https://doi:10.1016/j.exppara.2025.109028.

[10] Pan W, Hao WT, Shen YJ, *et al.*(2017) The excretory-secretory products of protoscoleces directly regulate the differentiation of B10, B17 and Th17 cells. Parasites & Vectors,10(1):348.https://doi:Artn 34810.1186/S13071-017-2263-9.

[11] Zhai S, Yang Y, Hu M, *et al.*(2026) Effect of LY2109761 on TGF-β1/TGFβRI/Smad Pathway and Hepatic Fibrosis Cysts Formation in Rats Infected with Echinococcus granulosus: an In Vitro and In Vivo Study. Acta Parasitologica,71(4).https://doi:10.1007/s11686-026-01324-y.

[12] Aimulajiang K, Chen X, Aizezi M, *et al.*(2026) The effects of protoscoleces proteins on host immune cells were elucidated through transcriptomic and metabolomic analyses. Veterinary Parasitology, 344(110755-110755.https://doi:Artn 11075510.1016/J.Vetpar.2026.110755.

[13] Vallerie AM, Lerner JP, Wright JD, *et al.*(2009) Peritoneal Inclusion Cysts A Review. Obstetrical & Gynecological Survey,64(5):321-334.https://doi:10.1097/OGX.0b013e31819f93d4.

[14] Anthony B, Allen JT, Li YS, *et al.*(2010) Hepatic stellate cells and parasite-induced liver fibrosis. Parasites & Vectors,3(1, article 60):1-7.https://doi:10.1186/1756-3305-3-60.

[15] Zhang CS, Wang LM, Ali T, *et al.*(2016) Hydatid cyst fluid promotes peri-cystic fibrosis in cystic echinococcosis by suppressing miR-19 expression. Parasites & Vectors,9(1).https://doi:Artn 27810.1186/S13071-016-1562-X.

[16] Luo G, Li H, Lu Q, *et al.*(2024) Effects of protoscoleces excretory-secretory products of Echinococcus granulosus on hepatocyte growth, function, and glucose metabolism. Acta Tropica,249(000):9. https://doi:10.1016/j.actatropica.2023.107066.

[17] Feng YY, Xu JY, Lu JX, *et al.*(2023) EgCF mediates macrophage polarisation by influencing the glycolytic pathway. Journal of Helminthology,97.https://doi:ARTN e10110.1017/S0022149X23000548.

[18] Wi?Niewski JR, Zougman A, Nagaraj N, *et al.*(2009) Universal sample preparation method for proteome analysis. Nature Methods,6(5):359-362.https://doi:10.1038/nmeth.1322.

[19] Gillet LC, Navarro P, Tate S, *et al.*(2012) Targeted Data Extraction of the MS/MS Spectra Generated by Data-independent Acquisition: A New Concept for Consistent and Accurate Proteome Analysis. Molecular & Cellular Proteomics,11(6):O111.016717.https://doi:Artn O111.01671710.1074/Mcp.O111.016717.

[20] Li Y, Link F, Fan W, *et al.*(2023) EGF/STAT1-maintained ECM1 expression in hepatic homeostasis is disrupted by IFNγ/NRF2 in chronic liver diseases. 39 Jahrestagung der Deutschen Arbeitsgemeinschaft zum Studium der Leber.2023.https://doi:10.1055/s-0042-1759918.

[21] Rostami-Rad S, Jafari R, Darani HY.(2018) Th1/Th2-type cytokine profile in C57 black mice inoculated with live protoscolices. Journal of Infection and Public Health,11(6):834-839.https://doi:10.1016/j.jiph.2018.06.007.

[22] Sato M, Muragaki Y, Ooshima A.(2005) TGF-β1/Smad3 Signaling in Renal Tubulointerstitial Fibrosis. Proceedings of The Japanese Society of Animal Models for Human Diseases,21:12-16.

[23] Qi XW, Shan JY, Liu XL, *et al.*(2021) The role of regulatory B cells in-infected mice. Parasitology Research,120(4):1389-1404.https://doi:10.1007/s00436-020-07025-3.

[24] Wang Y, X. YU, Z. LI, *et al.* Effect of TLR Signaling on IL-10-Producing Regulatory B cells. AADR Annual Meeting & Exhibition 2014; 2014.

[25] Díaz l.(2017) Immunology of cystic echinococcosis (hydatid disease). British Medical Bulletin,124(1):121-133.https://doi:10.1093/bmb/ldx033.

[26] Zhang Y, Yue Y, Cheng Y, *et al.*(2025) Antigen B from Echinococcus granulosus regulates macrophage phagocytosis by controlling TLR4 endocytosis in immune thrombocytopenia. Chemico-Biological Interactions,406.https://doi:10.1016/j.cbi.2024.111350.

[27] Jiang N, Chen Y, Li T, *et al.*(2024) Proteomic analysis of mouse liver lesions at all three stages of infection. Plos Neglected Tropical Diseases,18(12).https://doi:ARTN e001265910.1371/journal.pntd.0012659.

[28] Srivastava A, Evans KJ, Sexton AE, *et al.*(2017) Metabolomics-Based Elucidation of Active Metabolic Pathways in Erythrocytes and HSC-Derived Reticulocytes. Journal of Proteome Research,16(4):1492-1505.https://doi:10.1021/acs.jproteome.6b00902.

[29] Liu YH, Wu YY, Wang S, *et al.*(2026) Metabolomics-Based Elucidation of the Lipid-Lowering Mechanisms of Vinegar Polysaccharides. Foods,15(4).https://doi:Artn 65410.3390/Foods15040654.

[30] Tuerxun K, Abudoumijiti A, Yusupu Z*, et al.*(2010) Untargeted metabolomics reveals postoperative metabolic dynamics in hepatic cystic echinococcosis patients. Immunobiology,230(4):10.https://doi:10.1016/j.imbio.2025.153099.

[31] Xia X, Xia J, Yang H*, et al.*(2019) Baicalein blocked cervical carcinoma cell proliferation by targeting CCND1 via Wnt/β-catenin signaling pathway. Artificial Cells,47(1):2729-2736.https://doi:10.1080/21691401.2019.1636055.

[32] Zhu J, Zhao HQ, Aierken A*, et al.*(2024) Ghrelin is involved in regulating the progression of infected liver lesions through suppression of immunoinflammation and fibrosis. Plos Neglected Tropical Diseases,18(10).https://doi:ARTN e001258710.1371/journal.pntd.0012587.

[33] Ren B, Fan HN, Deng Y*, et al.*(2015) [Effect of Echinococcus multilocularis Cyst Fluid on the Expression of Five MAPK-pathway Genes of Rat Hepatic Stellate Cells]. Zhongguo Ji Sheng Chong Xue Yu Ji Sheng Chong Bing Za Zhi,33(2):114-117.

[34] Du X, Hua R, He X*, et al.*(2024) Echinococcus granulosus ubiquitin-conjugating enzymes (E2D2 and E2N) promote the formation of liver fibrosis in TGFβ1-induced LX-2 cells. Parasites & Vectors,17(1).https://doi:10.1186/s13071-024-06222-8.